Proceedings of ICMM2005
The 3rd International Conference on Microchannels and Minichannels
Toronto, Ontario, Canada, June 13-15, 2005

ICMM2005-75247

KINETIC MODELING OF TEMPERATURE DRIVEN FLOWS IN SHORT MICROCHANNELS

Alina A. Alexeenko
Department of Aerospace and Mechanical Engineering
University of Southern California
Los Angeles, California 90089
Email: alexeenk@usc.edu

Sergey F. Gimelshein*
Department of Aerospace and Mechanical Engineering
University of Southern California
Los Angeles, California 90089
Email: gimelshe@usc.edu

E. Phil Muntz
Department of Aerospace and Mechanical Engineering
University of Southern California
Los Angeles, California 90089
Email: muntz@spock.usc.edu

Andrew D. Ketsdever
Propulsion Directorate
Air Force Research Laboratory
Edwards Air Force Base, California 93524
Email: ketsdeve@spock.usc.edu

ABSTRACT

The temperature driven gas flow in a two-dimensional finite length microchannel and a cylindrical tube are studied numerically with the goal of performance optimization of a nanomembrane-based Knudsen compressor. The numerical solutions are obtained using direct simulation Monte Carlo method and discrete ordinate method for BGK model kinetic equation in a wide range of Knudsen numbers from 0.05 to 50. The length-to-height ratios from 5 to 30 were examined. Three different wall temperature distributions were considered, namely, linear, stepwise, and a non-monotonic profile typical for a radiantly heated Knudsen compressor membrane. The short channel end effects are characterized, and the sensitivity of the mass flow rate to a non-monotonic temperature distribution is shown.

INTRODUCTION

Lab on a chip technology is drawing the attention of scientists from many disciplines. Recent advances in MEMS manufacturing have made it possible to construct microscale analytical sensors such as integrated gas chromatography systems, miniature spectrometers, and mass spectrometers. The miniaturized detection devices will require microscale roughing pumps to provide sensor elements with gas samples at necessary environmental conditions. A pumping mechanism that can be exploited at microscale is thermal transpiration, a rarefied gas effect that drives the gas flow along the temperature gradient in a tube or channel. The main goal of this paper is the numerical study of thermal transpiration flows in short microchannels to aid in the performance optimization of a transpiration based microscale roughing pump known as the Knudsen compressor [1].

In early 1900s M. Knudsen built and studied the first transpiration based compressor, consisting of a series of differentially heated and cooled capillaries. Each stage of the compressor had a capillary section where the wall temperature increases, causing a thermomolecular pressure build-up at the high-temperature end of the capillary. The capillaries are followed by a connector stage of a significantly larger cross-sectional area, where the pressure is almost constant and temperature is decreased to its original value at the beginning of the stage. The modern version of Knudsen compressor was suggested by Pham-Van-Diep *et al* [2] and demonstrated by Vargo and Muntz [3]. The most critical element of the Knudsen compressor developed at USC is the thermal transpiration membrane made of porous materials, such as aerogel, with pore diameters on the order of the mean free

*Address all correspondence to this author.

Report Documentation Page

Form Approved
OMB No. 0704-0188

1. REPORT DATE	2. REPORT TYPE	3. DATES COVERED
MAR 2005		**-**

4. TITLE AND SUBTITLE	5a. CONTRACT NUMBER
Kinetic Modeling of Temperature Driven Flows in Short Microchannels	5b. GRANT NUMBER
	5c. PROGRAM ELEMENT NUMBER

6. AUTHOR(S)	5d. PROJECT NUMBER
A Alexeenko; S Gimelshein; E Muntz; A Ketsdever	**2308**
	5e. TASK NUMBER **0532**
	5f. WORK UNIT NUMBER

7. PERFORMING ORGANIZATION NAME(S) AND ADDRESS(ES)	8. PERFORMING ORGANIZATION REPORT NUMBER
Air Force Research Laboratory (AFMC),AFRL/PRSA,10 E. Saturn Blvd.,Edwards AFB,CA,93524-7680	

9. SPONSORING/MONITORING AGENCY NAME(S) AND ADDRESS(ES)	10. SPONSOR/MONITOR'S ACRONYM(S)
	11. SPONSOR/MONITOR'S REPORT NUMBER(S)

12. DISTRIBUTION/AVAILABILITY STATEMENT

Approved for public release; distribution unlimited

13. SUPPLEMENTARY NOTES

14. ABSTRACT

The temperature driven gas flow ina two-dimensional finite length microchannel and a cylindrical tube are studied numerically with the goal of performance optimization of a nanomembrane-based Knudsen compressor. The numerical solutions are obtained using direct simulation Monte Carlo method and discrete ordinate method for BGK model kinetic equation in a wide range of Knudsen numbers from 0.05 to 50. The length-to-height ratios from 5 to 30 were examined. Three differnt wall temperature distributions were considered, namely, linear, step-wise, and a non-monotonic profile typical for a radiantly heated Knudsen compressor membrane. The short channel end effects are characterized, and the sensitivity of the mass flow rate to a non-monotonic temperature distribution is shown.

15. SUBJECT TERMS

16. SECURITY CLASSIFICATION OF:			17. LIMITATION OF ABSTRACT	18. NUMBER OF PAGES	19a. NAME OF RESPONSIBLE PERSON
a. REPORT	b. ABSTRACT	c. THIS PAGE			
unclassified	**unclassified**	**unclassified**		**9**	

path of the gas at standard atmospheric conditions. The temperature gradient is maintained across the transpiration membrane by resistive or radiant heating. Recently, a single-chip micromachined implementation of a Knudsen pump was reported in Ref. [4], which can evacuate a cavity to 0.46 atm while operating at atmospheric pressure and using 80mW input power.

Knudsen compressor has several attractive features, such as no moving parts and no fluids or lubricants, and therefore, can have a number of promising applications provided that its performance can be optimized to meet the existing pumping requirements. The two most important performance parameters of the compressor are the energy use and volume per unit throughput. To accomplish minimization of these performance parameters the Knudsen compressor must also be designed to maximize the gas conductance through the device for a given temperature change. The required flow rate in the Knudsen compressor can be obtained by adjusting the cross-sectional area of the stages and the temperature distribution along the transpiration membrane at different stages. The main element of the transpiration based pump is rarefied gas flow through a capillary.

Rarefied gas flows of different gases through long tubes and channels were a topic of an extensive experimental and theoretical research over several decades, and a comprehensive review of the numerical data and analytical results for rarefied gas flows in capillaries was performed by Sharipov and Seleznev [5] (see also references therein). There is however a lack of reference data for nonisothermal flow through a capillary of a finite length, especially for arbitrary pressure and temperature drops.

The present numerical modeling of thermal transpiration flows in microchannels addresses several questions important for design optimization of Knudsen compressors, namely: the influence of different temperature internal distributions across the membrane on the flow field inside the capillaries and the total transpiration mass flow rates, the impact of the rarefaction on the capillary throughput, and capillary end effects.

Problem Statement

In the present work, two reservoirs filled with a single-species gas and joined by a two-dimensional capillary or a cylindrical tube of a finite length L and height h or radius a are considered in the computations. The two-dimensional channel configuration corresponds to the case of a capillary of infinite width w. A schematic of the geometric configuration and notations used throughout this paper are shown in Fig. 1. The subscripts I and II refer to the quantities attributed to the left and right container, respectively (far enough from the channel inlet and outlet). The channel walls have some temperature distribution varying from T_I to T_{II}. If the reservoirs are at the same temperature ($T_I = T_{II}$) and the pressure p_I is larger than p_{II} there will be a mass flow from the left container to the right one. Conversely, if the pressures are equal but a temperature drop is maintained between the reservoirs then the gas flow develops from the cold container to the hot one.

The summary of cases that have been considered is given in Table 1. The gas is molecular nitrogen in all simulations. The first set of computations (Cases I-a to I-e) is for a flow with both pressure and temperature gradients in a channel with a length-to-height ratio of 5 at different Knudsen numbers. Hereafter, the Knudsen number is based on the mean free path in the right reservoir and the channel height or tube diameter. Note also that the change in Knudsen number is due a change in the mean free path and not the capillary geometry. For each of these five cases we consider two different wall temperature distributions: linear and step-wise. In the second and third sets of calculations, the influence of different wall temperature distributions is examined for a channel and a tube, respectively, that connects reservoirs with a temperature ratio $T_I/T_{II} = 2$ and zero pressure drop (cases II-a to III-c).

DSMC Method

The DSMC method [6] has been applied in this work to obtain numerical solutions for short microchannel flows. The DSMC method is a statistical approach for solution of the Boltzmann equation, the governing equation of the rarefied flows. The DSMC method, initially proposed by G. A. Bird in the early 1960s, has become the most powerful and accurate method of numerical modeling of complex rarefied gas flows. [6] The fundamental principle of the DSMC method is the splitting of the dynamics of molecular motion during a time step Δt into two sequential stages: free-flight of molecules and intermolecular binary collisions. The DSMC method is non-stationary in nature, but can be used to solve stationary problems as well. Implementation of the DSMC method usually implies the discretization of the flow domain into a grid of cells. The size of computational cells should be sufficiently small so that the change in gas dynamic properties across each cell is small. In each cell, the Knudsen number based on the cell size should be larger than one. When the cell size in a simulation is too big, macroscopic gradients are typically underpredicted and the solution corresponds to an artificially larger Knudsen number. The time step in the simulation is usually selected such that $\Delta t = min(\tau_\lambda, \tau_{res})$, where τ_λ is the mean time between collisions, τ_{res} is the mean residence time in a cell, so that the molecules do not cross more than one cell during a time step. At each time step, the boundary conditions of the flow problem are modeled through particle injection at the domain boundaries and collisions with solid surfaces. After steady flow is reached, sampling of macroparameters within each cell is performed for a time period long enough to avoid statistical scatter.

The DSMC-based software SMILE [7] is used for all DSMC computations. The code uses the majorant frequency scheme [8] of the DSMC method for modeling of collisional process. The

intermolecular potential is assumed to be the variable soft sphere model [9]. The Larsen-Borgnakke model [10] with temperature-dependent Z_r and Z_v and discrete rotational and vibrational energies is used for the energy exchange between the translational and internal modes. At the gas-wall interface the the Maxwell model is used with the fully diffuse accommodation of tangential momentum and energy.

The background cell size in 2D DSMC calculations was 1/40th of the channel height, the the cell linear dimension is equal or less than the gas mean free path in all considered cases. The total number of background cells in each of the considered cases was 96,000. The average number of simulated molecules per background cell was 10. The total number of simulated molecules in the domain was about 1 million.

BGK Model Kinetic Equation Solution

The computational cost of DSMC simulations of low-speed flows in long channels becomes prohibitive due to low signal-to-noise ratio [11]. This is why for modeling of such flows it is reasonable to consider the solution of the steady-state Boltzmann equation with the collision operator simplified using BGK model [12],

$$U\frac{\partial f}{\partial x}+V\frac{\partial f}{\partial y}=\nu(f_0-f) \tag{1}$$

where $f(x,y,U,V,W)$ is the distribution function, x and y are Cartesian coordinates, U,V,W are velocity components, ν is the collision frequency and f_0 is the local equilibrium Maxwell-Boltzmann distribution function which depends on the moments of the distribution function f. This is a non-linear integrodifferential equation that uses a simplified form of the collision integral compared to the Boltzmann equation, and is applicable to model gas flows with arbitrary Knudsen numbers and degree of flow nonequilibrium.

The BGK model kinetic equation can be solved using a finite-difference method and standard discrete-ordinate method procedures [13, 14] for interpolation of the distribution function in velocity space. First, for the two-dimensional problems, reduced distribution functions are introduced:

$$g=\int_{-\infty}^{\infty} f\,dW, \quad h=\int_{-\infty}^{\infty} fW^2\,dW$$

One can introduce the polar coordinates in the velocity space as follows:

$$U=S\sin\phi, \qquad V=S\cos\phi.$$

The discrete speeds S_δ and velocity angles ϕ_σ:

$$n=\sum_\delta\sum_\sigma P_\delta P_\sigma g_{\delta\sigma}, \quad nU=\sum_\delta\sum_\sigma P_\delta P_\sigma S_\delta \sin\phi_\sigma g_{\delta\sigma}$$

$$nV=\sum_\delta\sum_\sigma P_\delta P_\sigma S_\delta \cos\phi_\sigma g_{\delta\sigma}, \quad \frac{3}{2}nT=\sum\sum P_\delta P_\sigma (h_{\delta\sigma}+S_\delta^2 g_{\delta\sigma})$$

Finally, the resulting system of equations

$$S_\delta \sin\phi_\sigma\frac{\partial g_{\delta\sigma}}{\partial x}+S_\delta\cos\phi_\sigma\frac{\partial g_{\delta\sigma}}{\partial y}=\nu(g^0_{\delta\sigma}-g_{\delta\sigma})$$

$$S_\delta \sin\phi_\sigma\frac{\partial h_{\delta\sigma}}{\partial x}+S_\delta\cos\phi_\sigma\frac{\partial h_{\delta\sigma}}{\partial y}=\nu(h^0_{\delta\sigma}-h_{\delta\sigma})$$

is solved by finite-difference method. The Gauss-Hermite half range quadrature [15] of order 16 and three-eights rule are used for integration over the speed and velocity angle, respectively.

Short Channel Flow under Temperature and Pressure Differences

The flow in the capillary section of a Knudsen compressor is driven by the temperature gradient in the presence of a small pressure gradient. In order to study separately the temperature effect, a temperature drop is assumed across the channel, with the density in the reservoirs being equal. Such flows through finite length channels in the presence of both temperature and pressure differences are examined in this section. The results presented in this section correspond to Cases I-a to I-e in Table 1. In all of the considered cases, the pressure ratio $P_I/P_{II}=1.5$ and temperature ratio is T_I/T_{II}=1.5. Since the pressure ratio in these cases exceeds the thermomolecular pressure ratio, there is a non-zero mass flow from the left reservoir to the right one. For each set of reservoir conditions two different temperature distributions are simulated, (1) a linear distribution from T_I to T_{II}, and (2) a step-wise distribution $T_w(x)=T_I$ for $x<L/2$; $T_w(x)=T_{II}$ for $x\geq L/2$. The stepwise temperature distribution may occur in Knudsen compressor if the transpiration membrane is composed of the materials with different thermal conductivities.

The calculated gas translation temperature and X-component of the velocity fields are shown in Figs. 2 and 3, respectively, for Cases I-c ($\mathrm{Kn}_I I$=1) and I-e (Kn_{II}=0.05). The temperature gradients are less steep for Case I-c than for Case I-e due to larger mean free path. The end effects are apparent in the velocity field and result in an effective elongation of the

channel. The most important conclusion that may be drawn from these figures is that the temperature distribution does not impact the flow outside of the channels. This is true for both Knudsen numbers considered. Moreover, the velocity fields for the linear and step-wise temperature distributions are close near the surface, but differ significantly at the centerline.

Comparison of density profiles along the centerline for the above cases is given in Fig. 4. General behavior of density profiles is similar for different Knudsen numbers and temperature variation, with density being lower in the high-temperature part, and higher in the low-temperature part. This is related to a relatively lower thermal velocities of the latter and, as the result, their longer residence time and larger densities. Similarly, the population of molecules in the high temperature region is affected by short residence times in that region. This effect is obviously more pronounced in the step distribution cases. The molecular collisions increase the deviation of density from its average value.

The X-component of velocity profile along the centerline is plotted in Fig. 5. The pressure-driven Poiseuille and temperature-driven thermal creep flows represent two competing flow mechanisms in these cases. Due to the thermal creep flow from the cold container to the hot one, the X-component of velocity is lower in Cases I-e (lin) and I-e (step) than in the case of no temperature gradient. In the case of step-wise wall temperature distribution, the resulting velocity profile in the channel is non-monotonic, and has a strong gradient in the step region due to thermal creep.

The calculated mass flow rates for Cases I-a to I-e are listed in Table 2. The flow coefficients Q_P and Q_T are used here that are usually employed for characterization of the Poiseuille and thermal creep flows between parallel plates for the conditions of small temperature and pressure gradients. The flow coefficients are defined as follows:

$$Q_P = \frac{\dot{M}}{(\frac{1}{2}\sqrt{2RT_0})\rho_0 wh^2 \frac{1}{p_0}\frac{\Delta p}{L}}, \qquad Q_T = \frac{\dot{M}}{(\frac{1}{2}\sqrt{2RT_0})\rho_0 wh^2 \frac{1}{T_0}\frac{\Delta T}{L}} \tag{2}$$

where $\dot{M}$ is the mass flow rate (kg/s), ρ_0, p_0, and T_0 are the average density, pressure, and temperature, respectively, and w, h, L are channel width, height and length, respectively. There is no significant difference in the mass flow rate between the linear and stepwise temperature distributions. In fact, the difference in mass flow rate is less than 2 per cent for all Knudsen numbers.

Influence of Wall Temperature Distribution

Temperature gradient driven flows are very sensitive to thermal boundary conditions. For practical microdevices it is generally difficult to attain idealized thermal boundary requirements. Thus, numerical methods for reliably estimating the magnitude of the consequences induced by non-ideal conditions are important.

As an illustration of the usefulness of this approach consider the recent development by Young [16] of a prototype Knudsen Compressor. Radiant energy was used to generate temperature gradients in the carbon doped aerogel membranes that are the active elements in the compressor's pumping stages. Due to finite photon mean free paths in the carbon doped aerogel membranes, the wall temperatures in the membrane's flow passages had a maximum near to, but not at, the exit surface of the membrane. This is the motivation for the calculations in this section with the non-monotonic wall temperature variation of case III-c (see table 1) constructed to mimic the essentials of a membrane in Young's experiments.

The influence of wall temperature distribution on the thermal transpiration flow in short microchannel was considered for a channel with length-to-height ratio of 5 at Kn_{II}=0.2. To study this effect, the pressure was assumed equal in the two reservoirs, and the temperature drop was set to 300 K. The three cases of temperature distribution are (i) the linear temperature variation along the channel wall (case II-a), (ii) a step-wise temperature variation (case II-b) and (iii) a non-monotonic distribution typical for a radiatively heated nanomembrane Knudsen compressor [16] (case II-c). A non-monotonic wall temperature profile has a maximum of 750 K at one-fourth of the channel length. The three wall temperature distributions are plotted in Fig. 6.

The change in the wall temperature distribution significantly impacts the flow velocity (see Fig. 8). Note that only a portion of computational domain is shown to illustrate the details of the flow inside the channel. This impact is noticeably stronger that the one shown in the previous section, and is observed both at the centerline and near the surface.

The influence of wall temperature distributions inside the channel on the temperature field is illustrated in Fig. 7. The gas temperature generally follows the surface temperature inside the channel, with the end effects being visible even at a distance from the inlet/outlet equal to the channel length. The end effects are somewhat smaller for the stepwise distribution, and largest for the non-monotonic profile.

Figure 9 shows the calculated pressure profiles along the centerline for the above temperature distributions. The qualitative behavior is similar for the linear and stepwise distribution, with pressure larger in the hot part, and smaller in the cold part. The non-monotonic case significantly differs from the first two, since there is no significant pressure minimum in the cold part. Also, there is a pressure increase inside the channel of about 10 percent for the monotonic profile due to the reverse transpiration.

The calculated mass flow rate and flow coefficient Q_T for the three cases are listed in Table 3. The mass flow rate in case of stepwise temperature variation is only slightly lower (by $\approx 3\%$) than for the linear temperature variation. However, the reverse transpiration in the non-monotonic temperature distribution case

results in significant degradation of mass throughput (by $\approx 18\%$).

Similar influence of the wall temperature distribution is observed for a cyllindrical tube case (see Table 4). The decrease of the mass flow rate is close to that for a two-dimensional case and is equal to about 2% and 17% for stepwise and non-monotonic wall temperature distributions, respectively.

Validation of the BGK Solver

Results of the validation study of a channel flow modeling using a BGK model kinetic equation are presented in this section. The solutions obtained using the BGK solver are compared with the solution of Navier-Stokes equations for long channels at low Knudsen number and a DSMC solution for a short channel in the transitional regime.

1) *Comparison with Navier-Stokes solution* The flow of nitrogen in a channel with a length-to-height ratio of 30 was calculated for a pressure ratio of 1.5 and a constant temperature of the wall of 300 K. The temperature in the upstream and downstream reservoirs is equal to 300 K. The Knudsen number based on the channel height and the mean free path in the downstream reservoir is 0.05.

The X-component of velocity field is shown in Fig. 10 obtained using three different uniform spatial grids in the BGK solver. The grid dimensions are: (i) 101x51, (ii) 51x26 and (iii) 26x14. The analytical approximate solution [17] of Navier-Stokes equations for a long channel flow with slip boundary conditions is also plotted in Fig.10. The discrete ordinate solution of BGK model kinetic equation with coarser grids results in a lower velocity in the whole computational domain. Note that a similar dependence of results on the number of simulated particles and cells in the DSMC method was observed [18]. The solution obtained for a 101x51 grid is in excellent agreement with the Navier-Stokes solution.

2) *Comparison with a DSMC solution* The flow of nitrogen in a short channel with a length-to-height ratio of 5 was calculated for a pressure ratio of 1.5 and a constant wall temperature of 300 K. The Knudsen number based on the channel height and the mean free path in the downstream reservoir is 0.2, resulting in a transitional flow regime in the channel.

Figure 11 shows a comparison of X-component of velocity profiles in the channel obtained by the BGK solver (top) and a DSMC solver SMILE (bottom). Overall, the two solutions are in a very good agreement with the maximum difference in the velocity values at the axis of about 2% which is within the error of both numerical methods.

Thus, the area of applicability of the BGK model kinetic equation for numerical modeling of microchannel flows spans a wide range of flow regimes: from near-continuum to rarefied, as well as different geometries: both small and large length-to-height ratios, and arbitrary pressure gradients between the reservoirs.

Conclusions

The direct simulation Monte Carlo method and the discrete ordinate method for the solution of the BGK model were used to numerically study rarefied gas flows through two-dimensional finite length channels. A wide range of flow rarefaction regimes was examined, from Kn=0.05 to 50, in the presence of pressure and/or temperature gradients. Three different wall temperature distributions were considered, namely, linear, step-wise, and a non-monotonic profile typical for a radiantly heated Knudsen compressor membrane.

The influence of wall temperature distribution on the thermal transpiration flow in a short channel at Kn_{II}=0.2 was considered. The non-monotonic wall temperature distribution case significantly differs from the first two. There is a pressure increase inside the channel of about 10 percent for the non-monotonic profile due to the reverse transpiration. The mass flow rate in case of stepwise temperature variation is only slightly lower (by 3%) than for the linear temperature variation. However, the reverse transpiration caused by the non-monotonic wall temperature distribution results in significant degradation of mass flow, by about 18%. Similar influence of the wall temperature distribution is observed for a cyllindrical tube case.

The application of the numerical techniques discussed in this paper to detailed investigations and optimizations of microscale thermal creep flows will be extremely valuable. The work reported here is a first look at describing practical thermal gradient driven or thermal creep flows. While the available results are at present both scarce and preliminary, they do validate in this case what was anticipated, and provide useful quantitative estimates of the consequences of the particular wall temperature maximum chosen for the calculations.

REFERENCES

[1] Knudsen, M., 1910. "Eine revision der gleichgewichtsbedingung der gase. thermische molecularstr'omung". *Ann. Phys., Leipzig*, **31**.

[2] Pham-Van-Diep, G., Keeley, P., Muntz, E. P., and Weaver, D. P. "A micromechanical Knudsen compressor". In *Rarefied Gas Dynamics*. eds. J. Harvey, G. Lord, Oxford University Press, Oxford,.

[3] Vargo, S. E., and Muntz, E. P., 1997. "An evaluation of a multiple stage micromechanical Knudsen compressor and vacuum pump". In *Rarefied Gas Dynamics*. eds. Ching Shen, Peking University Press, Beijing, pp. 995–1000.

[4] McNamara, S., and Gianchandani, Y. B., 2003. "A micromachined Knudsen pump for on-chip vacuum". In *Proceedings of the 12th International Conference on Solid State Sensors, Actuator and Microsystems, Boston, MA*, Vol. 2. pp. 1919–1922.

[5] Sharipov, F., and Seleznev, V., 1998. "Data on internal rar-

efied gas flows". *J. Phys. Chem. Ref. Data*, **27**(3), pp. 657–706.

[6] Bird, G. A., 1994. *Molecular Gas Dynamics and the Direct Simulation of Gas Flows*. Clarendon Press, Oxford.

[7] Ivanov, M. S., Markelov, G. N., and Gimelshein, S. F., 1998. "Statistical simulation of reactive rarefied flows: Numerical approach and applications". *AIAA Paper 98-2669*.

[8] Ivanov, M. S., and Rogasinsky, S. V., 1988. "Analysis of numerical techniques of the direct simulation Monte Carlo method in the rarefied gas dynamics". *Sov. J. Numer. Anal. Math. Modeling*, **3**(6), pp. 453–465.

[9] Koura, K., and Matsumoto, H., 1991. "Variable soft sphere molecular model for inverse-power-law of Lennard-Jones potential". *Phys. Fluids A*, **3**(10), pp. 2459–2465.

[10] Borgnakke, C., and Larsen, P. S., 1975. "Statistical collision model for Monte Carlo simulation of polyatomic gas mixture". *J. Comp. Phys.*, **18**, pp. 405–420.

[11] Cai, C., Boyd, I. D., Fan, J., and Candler, G. V., 2000. "Direct simulation methods for low-speed microchannel flow". *J. Thermophysics and Heat Transfer*, **14**(3), pp. 368–378.

[12] Bhatnagar, P., Gross, E., and Krook, M., 1954. "A model for collision processes in gases. i. small amplitude processes in charged and neutral one-component systems". *Phys. Rev.*, **94**(3), pp. 511–525.

[13] Cercignani, C., 1975. *Theory and Application of the Boltzmann Equation*. Elsevier, New York.

[14] Chung, C., and Wereley, S., 2003. "Analysis of gas flows in microchannels with small pressure difference". *AIAA Paper 2003-861*.

[15] Shizgal, B., 1981. "A gaussian quadrature procedure for use in the solution of the Boltzmann equation and related problems". *J. Comp. Physics*, **41**, pp. 309–328.

[16] Young, M., 2004. "Investigation of several important phenomena associated with the development of Knudsen compressors". PhD thesis, University of Southern California.

[17] Arkilic, E. B., Schmidt, M. A., and Breuer, K. S., 1997. "Gaseous slip flow in long microchannels". *J. of MEMS*, **6**(2), June, pp. 167–178.

[18] Alexeenko, A., Gimelshein, S., and Levin, D., 2003. "Reconsideration of flows through constriction microchannels using the dsmc method". *AIAA Paper 2003-4009*.

Table 1. Summary of cases considered

Flow Conditions	Designation
Pressure and Temperature-Driven Flow	
L/h=5, N_2, T_I=600 K, T_{II}=300 K, $\frac{p_I}{p_{II}}$=1.5	
Kn_{II}=50	*case I-a*
Kn_{II}=3	*case I-b*
Kn_{II}=1	*case I-c*
Kn_{II}=0.2	*case I-d*
Kn_{II}=0.05	*case I-e*
Effect of Wall Temperature Distribution	
Two-dimensional channel:	
L/h=5, Kn_{II}=0.2, N_2, T_I=600 K, T_{II}=300 K, $\frac{p_I}{p_{II}}$=1.0	
linear	*case II(lin)*
step	*case II(step)*
non-monotonic	*case II(nmon)*
Axisymmetric tube:	
L/a=5, Kn_{II}=0.2, N_2, T_I=600 K, T_{II}=300 K, $\frac{p_I}{p_{II}}$=1.0	
linear	*case III(lin)*
step	*case III(step)*
non-monotonic	*case III(nmon)*

Table 2. Calculated mass flow rate and flow coefficients for pressure and temperature driven flow in short channel.

Case	$\dot{m}$ (kg/s)	Q_P	$\frac{\dot{m}}{\Delta p} \times 10^7$ ($kg/s \cdot Pa$)
I-a (lin)	0.119×10^{-7}	0.533	2.17
I-a (step)	0.119×10^{-7}	0.533	2.17
I-b (lin)	0.229×10^{-6}	0.615	2.5
I-b (step)	0.229×10^{-6}	0.615	2.5
I-c (lin)	0.812×10^{-6}	0.727	2.96
I-c (step)	0.824×10^{-6}	0.738	3.0
I-d (lin)	0.672×10^{-5}	1.20	4.90
I-d (step)	0.677×10^{-5}	1.21	4.93
I-e (lin)	0.555×10^{-4}	2.49	10.11
I-e (step)	0.554×10^{-4}	2.48	10.09

Table 3. Calculated mass flow rate and flow coefficient for temperature-driven flow in short channel, Case II.

Temperature Distribution	$\dot{m}$ (kg/s)	Q_T
linear	1.580E-6	0.1189
stepwise	1.532E-6	0.1153
non-monotonic	1.292E-6	0.0972

Table 4. Calculated mass flow rate and flow coefficient for temperature-driven flow in short tube, Case III.

Temperature Distribution	$\dot{m}$ (kg/s)	Q_T
linear	1.06E-9	0.1269
stepwise	1.04E-9	0.1245
non-monotonic	8.8E-10	0.1054

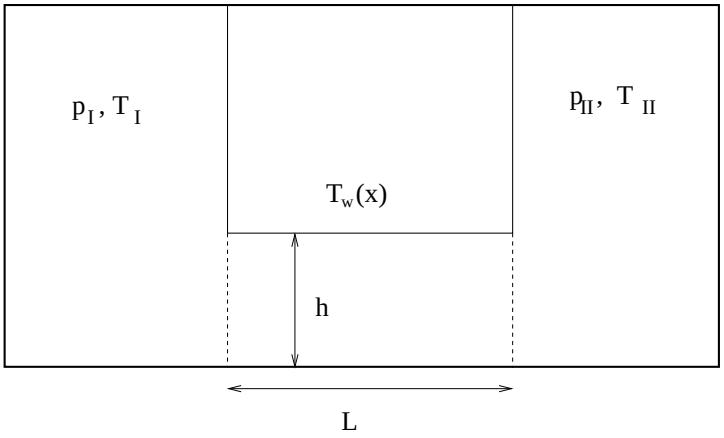

Figure 1. Schematic of the problem and notations.

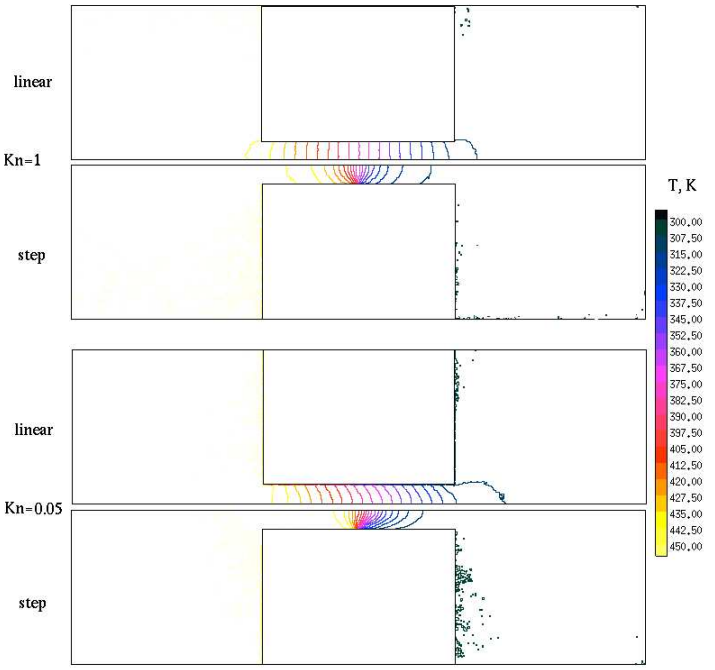

Figure 2. Translational temperature field for Cases I-c and I-e.

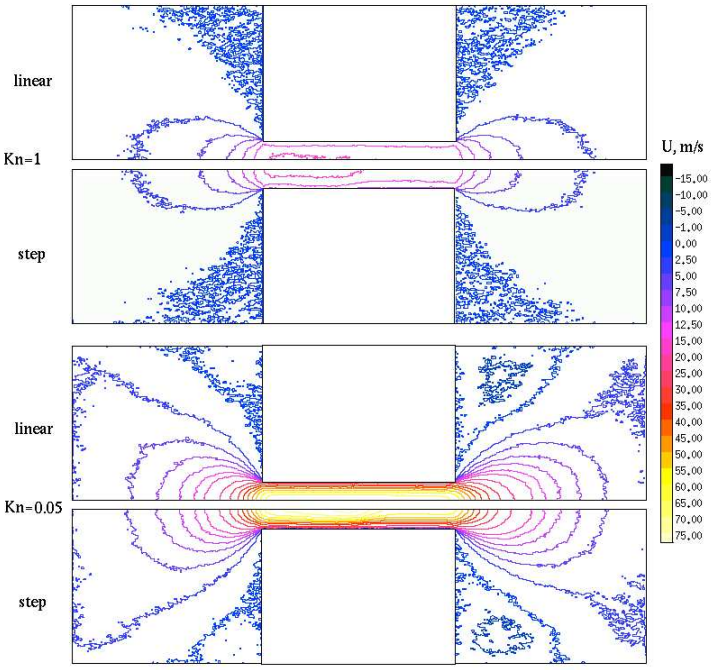

Figure 3. X-component of velocity field for Cases I-d and I-e.

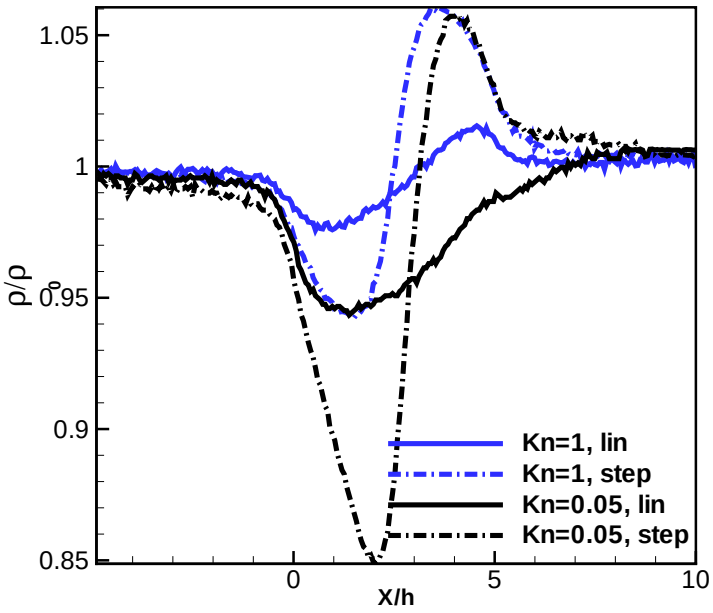

Figure 4. Normalized density profile along the channel for different temperature variations and Knudsen numbers (Cases I-c and I-e).

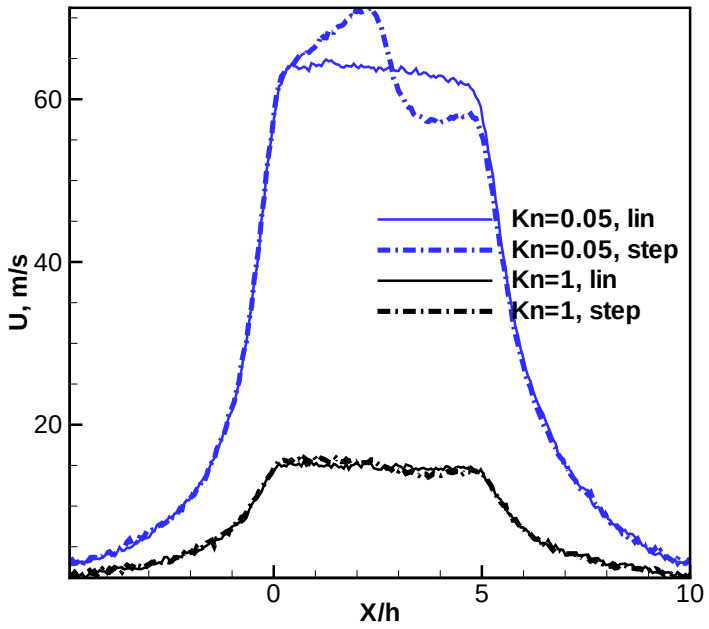

Figure 5. X-component of velocity profile along the channel for different temperature distributions and Knudsen numbers (Cases I-c and I-e).

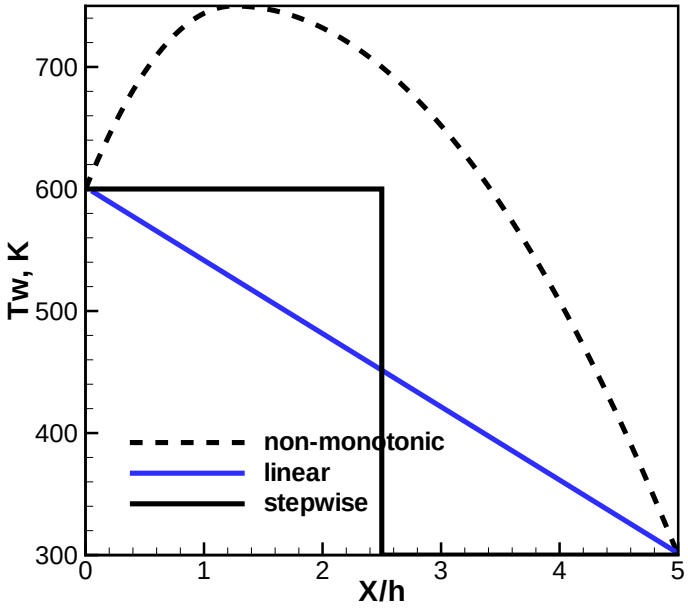

Figure 6. Wall temperature distributions for Case II.

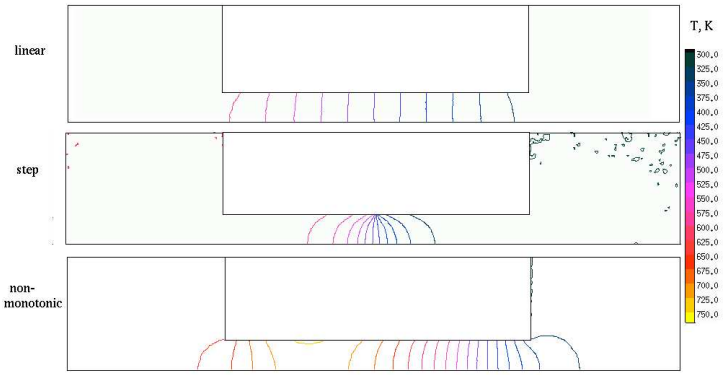

Figure 7. Translational temperature field, Kn_{II}=0.2, L/h=5 for different temperature variations, Case II

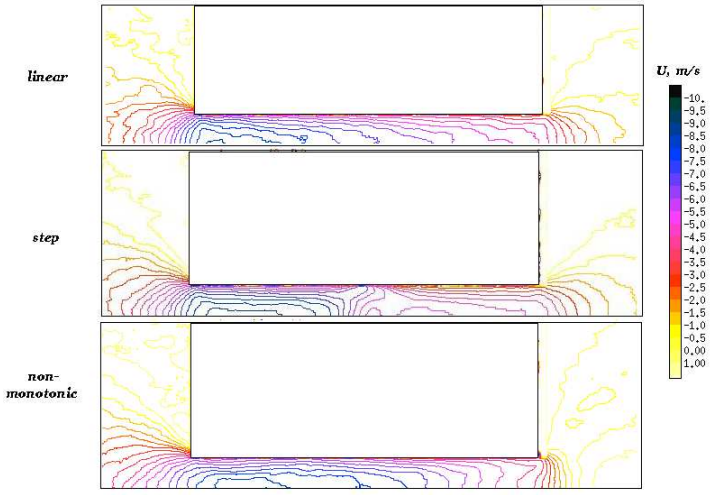

Figure 8. X-component of velocity field, Kn_{II}=0.2, L/h=5 for different temperature variations, Case II

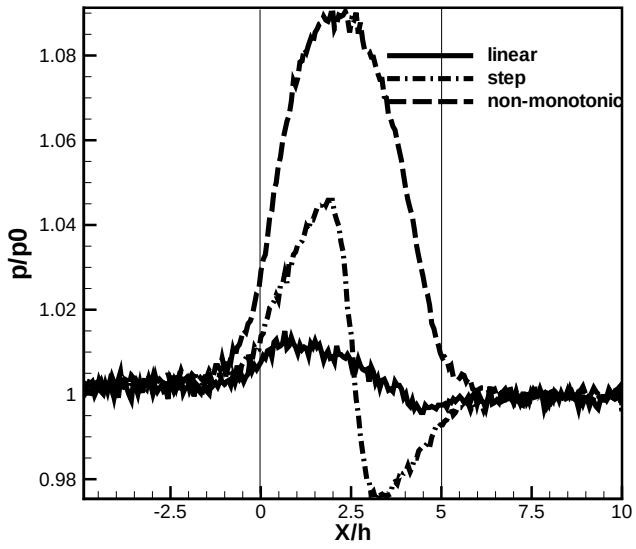

Figure 9. Pressure profile along the channel, Kn_{II}=0.2, L/h=5 for different temperature variations, Case II.

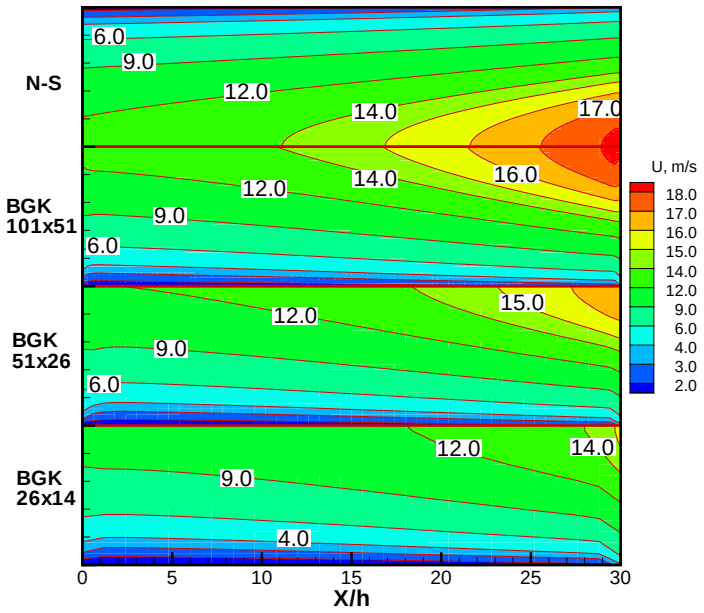

Figure 10. Comparision of X-component of velocity field calculated using Navier-Stokes equations (top) and BGK model with different meshes, Kn_{II}=0.05, L/h=30.

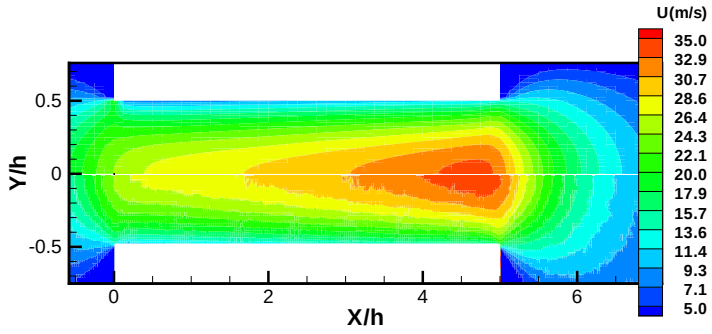

Figure 11. Comparison of X-component of velocity field calculated using BGK(top) and DSMC (bottom) models, Kn_{II}=0.2, L/h=5.